J|A|C|S
ARTICLES
Published on Web 08/16/2002

Rigid Dendritic Donor−Acceptor Ensembles: Control over Energy and Electron Transduction

Dirk M. Guldi,*,† Angela Swartz,† Chuping Luo,† Rafael Gómez,‡ José L. Segura,*,‡ and Nazario Martín*,‡

Contribution from the Radiation Laboratory, University of Notre Dame, Indiana 46556, and Departamento de Química Orgánica, Facultad de Química, Universidad Complutense, E-28040 Madrid, Spain

Received December 12, 2001. Revised Manuscript Received June 26, 2002

Abstract: Several generations of phenylenevinylene dendrons, covalently attached to a C_{60} core, have been developed as synthetic model systems with hierarchical, fine-tuned architectures. End-capping of these dendritic spacers with dibutylaniline or dodecyloxynaphthalene, as antennas/electron donors, yielded new donor−bridge−acceptor ensembles in which one, two, or four donors are allocated at the peripheral positions of the well-defined dendrons, while the electron accepting fullerene is placed at the focal point of the dendron. On the basis of our cyclic voltammetry experiments, which disclose a single anodic oxidation and several cathodic reduction processes, we rule out significant, long-range couplings between the fullerene core and the end-standing donors in their ground-state configuration. Photophysical investigations, on the other hand, show that upon photoexcitation an efficient and rapid transfer of singlet excited-state energy (6×10^{10} to 2.5×10^{12} s^{-1}) controls the reactivity of the initially excited antenna portion. Spectroscopic and kinetic evidence suggests that yet a second contribution, that is, an intramolecular electron-transfer, exists, affording $C_{60}^{\bullet-}$ −dendron$^{\bullet+}$ with quantum yields (Φ) as high as 0.76 and lifetimes (τ) that are on the order of hundreds of nanoseconds (220−725 ns). Variation of the energy gap modulates the interplay of these two pathways (i.e., competition or sequence between energy and electron transfer).

Introduction

Cascades of light-driven energy and electron-transfer processes, along well-defined energy and redox gradients, bear key character in biology, chemistry, and materials science.[1] Inspired by the complex function of photosynthesis, that is, light harvest by the antenna ensemble, transduction of excitation energy to the photosynthetic reaction center, and charge-separation thereafter, numerous artificial model systems have been devised.[2] Understanding the parameters that dictate, for instance, the mutual interplay between efficient energy migration and unidirectional electron transfer is a long-standing objective. A crucial contention in this debate is to determine the factors that activate these fundamentally different processes in a synchronous (i.e., competition) or, alternatively, in an antichronous manner (i.e., sequence). In the event of a sequential scenario, optimizing each of the associated relay steps emerges as a multifaceted and complex task. In principle, an optimal synergism necessitates combining an appropriate energy gap with an adequate spacing and orientation to contrive a good-performing solar energy conversion system.[3]

One of the most common problems in artificial model systems is the lack of efficient solar light capture, because of insufficient chromophore activity. To overcome this intrinsic limitation, integration of several chromophores in "series" or "parallel" holds particular promise for increased absorptive cross sections and, thus, an efficient use of the solar spectrum. The strategy of choice implies well-defined core−shell ensembles, in which assemblies of chromophores are integrated in a "parallel" configuration. This "parallel" design provides an enormous advantage: The topography, that is, a central core surrounded by a shell of chromophores, facilitates the mutual electronic coupling with each individual constituent.

The intervening spacer is essential to guarantee the control over the separation, electronic coupling, and composition in donor−acceptor assemblies.[4,5] Importantly, dendritic structures, bearing an electro- and/or photoactive interior core, a closed-packed shell, and a highly functional surface, furnish key criteria, such as structural rigidity and long-range conjugation. Some of their most fascinating features reach out to light-harvesting arrays and electron-transfer relays of different complexities (i.e., enhancing the molecular function with increasing generation).

* To whom correspondence should be addressed. E-mail: guldi.1@nd.edu (D.M.G.); nazmar@quim.ucm.es (N.M.).
† University of Notre Dame.
‡ Universidad Complutense.

(1) (a) Balzani, V.; Scandola, F. *Supramolecular Photochemistry*; Ellis Horwood: Chichester, U.K., 1991; pp 161−196, 355−394. (b) Turro, N. J. *Modern Molecular Photochemistry*; University Science Books: Mill Valley, CA, 1991; pp 321−361. (c) Speiser, S. *Chem. Rev.* **1996**, *96*, 1953.
(2) Gust, D.; Moore, T. A.; Moore, A. L. *Acc. Chem. Res.* **2001**, *34*, 40 and references therein
(3) Wasielewski, M. R. *Chem. Rev.* **1992**, *92*, 435.
(4) (a) Fox, M. A.; Chanon, M. *Photoinduced Electron Transfer*; Elsevier: Amsterdam, 1988. (b) Balzani, V. *Electron Transfer in Chemistry Vol. I−V*; Wiley-VCH: Weinheim, Germany, 2001. (c) Carter, F. L. *Molecular Electronic Devices*; Marcel Dekker: New York, 1987.
(5) (a) Stowell, M. H. B.; McPhillips, T. M.; Rees, D. C.; Soltis, S. M.; Abresch, E.; Feher, G. *Science* **1997**, *276*, 812. (b) McDermott, G.; Prince, S. M.; Freer, A. A.; Hawerthornthwaite-Lawlwss, A. M.; Paiz, M. Z.; Cogdell, R. J.; Isaacs, N. W. *Nature* **1995**, *374*, 517.

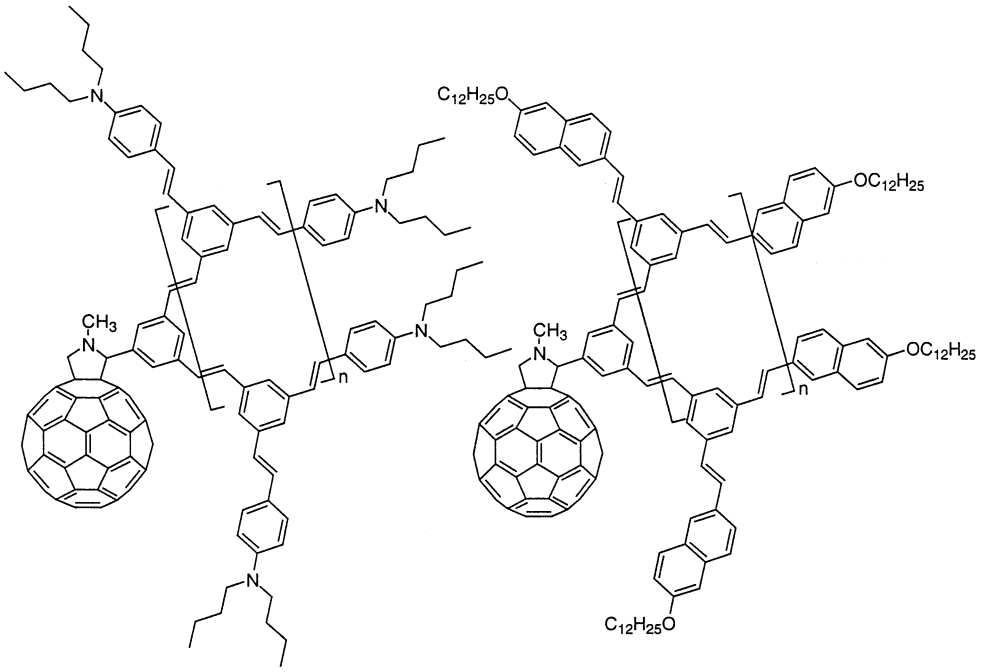

Figure 1. First (**1a**, **1b**) and second (**2a**, **2b**) generations of new C_{60}−dendron dyads.

The features of the dendron skeleton can be fine-tuned at a molecular level not only within a simple two-component system (i.e., one donor−one acceptor) but, most significantly, within multicomponent ensembles (i.e., several donors−one acceptor), which ultimately can lead to high solar energy conversion efficiencies.[6]

Previous work has focused mainly on encapsulating flexible dendron units.[7] Their overall flexibility precludes, however, meaningful conclusions on effects that may relate to distance and coupling between the donor and acceptor couples. Considering this deficiency, we drew our attention to the unique features of stiff dendritic macromolecules.[8] Their convergent constitution facilitates the construction of well-defined energy gradients via a site-specific functionalization. In turn, energy might be funneled from, for example, an array of light-collecting chromophores at the periphery toward a single energy/electron "sink" in the core.

The spherical shape of fullerenes, giving rise to a delocalized π-electron system, renders these carbon allotropes ideal components for the construction of efficient electron-transfer model systems. The delocalization of charges, electrons or holes, within the giant, spherical carbon framework (diameter > 7.5 Å), together with the rigid, confined structure of the aromatic π-sphere, offers unique opportunities for stabilizing charged entities. Most importantly, the small reorganization energy, found for C_{60} in electron-transfer processes, accelerates the initial charge-separation and shifts the strongly exothermic charge recombination deep into the "inverted-region" decelerating its rate. In fact, efficient relays of electron-transfer reactions, for example, in fullerene-based dyad, triad, and tetrad ensembles, has been accomplished along well-designed and fine-tuned redox gradients leading to lifetimes as long as 0.38 s.[9]

In this paper, we describe several new D−B−A (donor−bridge−acceptor) systems in which one (**19**), two (**1a**), or four (**2a**) dibutylaniline or dodecyloxynaphthalene (**1b**, **2b**) electron donors are located at the peripheral positions of well-defined phenylenevinylene-based dendrons and a fullerene acceptor at the focal point of the dendrimer (Figure 1). Most importantly, pursuing this strategy helps to alter the absorption cross section of the antenna portion, that is, the dibutylaniline or dodecyloxynaphthalene periphery. We will demonstrate that, in these model systems, modulation of the energy gap and the relative energetic positioning of the states involved leads alternatively to a sequence or a competition in energy- and electron-transfer reactions. As far as the different generations of dendrons are concerned, their rigid constitution creates diverse donor−acceptor separation ranging from 8.56 Å (**17**) to 19.1 Å (**2b**).

Results

Synthesis. Synthesis of Functionalized Phenylenevinylene-Based Dendrons. The synthetic procedure for the preparation of C_{60}−dendron dyads is based on the 1,3-dipolar cycloaddition reaction[10] of C_{60} with aldehyde-functionalized dendrons. Therefore, the target molecules for our synthetic workup are phen-

(6) For reviews on light-harvesting and photoactive dendrimers see: (a) Adronov, A.; Fréchet, J. M. J. *Chem. Commun.* **2000**, 1701. (b) Venturi, M.; Serroni, S.; Juris, A.; Campagna, S.; Balzani, V. *Top. Curr. Chem.* **1998**, *197*, 193. (c) Vogtle, F.; Gestermann, S.; Hesse, R.; Schwierz, H.; Windisch, B. *Prog. Polym. Sci.* **2000**, *25*, 987.

(7) (a) Nierengarten, J.-F. *Chem.—Eur. J.* **2000**, *6*, 3667. (b) Hirsch, A.; Vostrowsky, O. *Top. Curr. Chem.* **2001**, *217*, 51.

(8) (a) Xu, Z.; Moore, J. S. *Acta Polym.* **1994**, *45*, 83. (b) Devadoss, C.; Bharathi, P.; Moore, J. S. *J. Am. Chem. Soc.* **1996**, *118*, 9635. (c) Shortreed, M. R.; Swallen, S. F.; Shi, Z.-Y.; Tan, W.; Xu, Z.; Devadoss, C.; Moore, J. S.; Kopelman, R. *J. Phys. Chem. B* **1997**, 101, 6318. (d) Swallen, S. F.; Shi, Z.-Y.; Tan, W.; Xu, Z.; Moore, J. S.; Kopelman, R. *J. Lumin.* **1998**, *76*−*77*, 193. (e) Avent, A. G.; Birkett, P. R.; Paolucci, F.; Roffia, S.; Taylor, R.; Wachter, N. K. *J. Chem. Soc., Perkin Trans. 2* **2000**, 1409. (f) Segura, J. L.; Gómez, R.; Martín, N.; Luo, C.; Swartz, A.; Guldi, D. M. *Chem. Commun.* **2001**, 707.

(9) Imahori, H.; Guldi, D. M.; Tamaki, K.; Yoshida, Y.; Luo, C.; Sakata, Y.; Fukuzumi, S. *J. Am. Chem. Soc.* **2001**, 123, 6617.

(10) Prato, M.; Maggini, M. *Acc. Chem. Res.* **1998**, *31*, 519.

Scheme 1

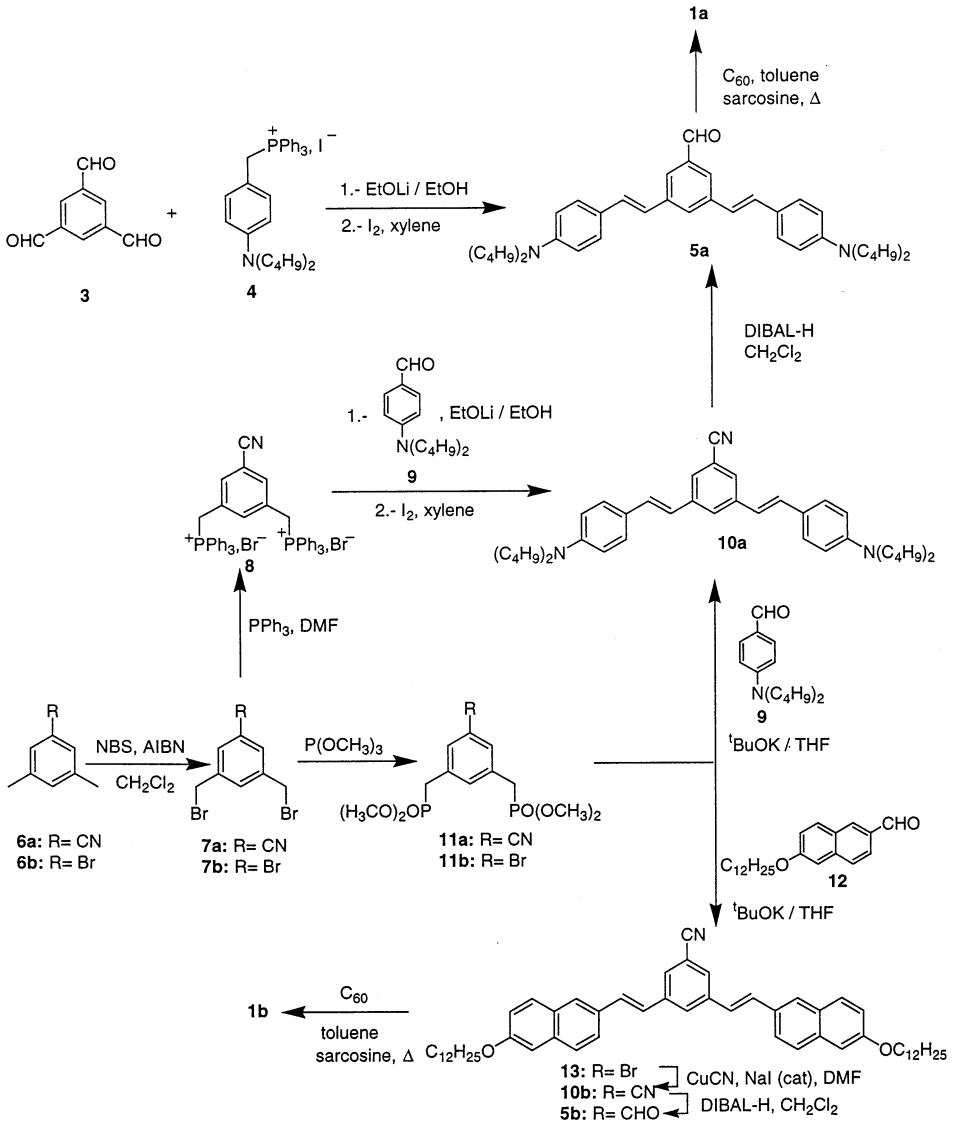

ylenevinylene-based dendrons carrying aldehyde functionalities at their focal point. Three different synthetic routes (Scheme 1) were pursued to get to the first generation dendron **5a**, carrying the required aldehyde functionality.

Access to the second-generation dendron **14a**, with a nitrile functionality at the focal point, was made possible by the Wittig−Horner reaction between bis(phosphonate) **11a** and aldehyde **5a**. Subsequent treatment of **14a** with a stoichiometric amount of 1.0 M solution of DIBAL-H (diisobutylaluminum hydride) in dichloromethane furnished **15a** as a yellowish solid in a 78% yield (Scheme 2).

The good solubility of these compounds guaranteed full spectroscopic characterization of the new dendrons. The FTIR spectra show the fingerprints of the functional groups present at the focal point: A band around 2220 cm^{-1} corresponds in **10a** and **14a** to the conjugated nitrile group, while in **5a** and **15a** a band at lower frequencies (1690 cm^{-1}) represents the aldehyde functionality.

The ^1H NMR spectra for the *E*,*E* isomer (**5a**) show the signal corresponding to the aldehyde group (9.98 ppm) together with two other signals as singlets corresponding to the central benzene moiety (7.79 and 7.76 ppm). The remaining hydrogen atoms of the peripheral benzene rings are grouped into an AA′BB′ system with a coupling constant (*J*) of 8.8 Hz. On the other hand, the olefinic protons give rise to two doublets with a coupling constant of 16.4 Hz, which provides further proof for their *E* configuration. Similar δ values and coupling constants for the peripheral benzene rings and the olefinic protons were noted in the higher generation dendrimers. In addition, a series of new signals were assigned to the inner benzene rings. The alkyl chains give rise to a triplet at 3.2 ppm and several multiplets, corresponding to the methylene group directly attached to the nitrogen atoms, and the remaining methylene and methyl groups, respectively.

In the ^{13}C NMR spectra, the signals associated with the aromatic carbon atoms (i.e., carrying the dibutylamino groups) appear around 147 ppm. The rest of the signals observed are in agreement with the proposed structures which are also confirmed by mass spectrometry (**5a**: M^+ 564; **15a**: M^+ 1228) and elemental analyses.

Synthesis of C_{60}−Dendron. Treating aldehydes (**5a**,**b** and **15a**,**b**) with [60]fullerene and an excess of sarcosine in refluxing toluene for 24 h gave C_{60}−dendron dyads (**1a**,**b** and **2a**,**b**) (see Schemes 1 and 2). Because of the presence of the long alkyl

Scheme 2

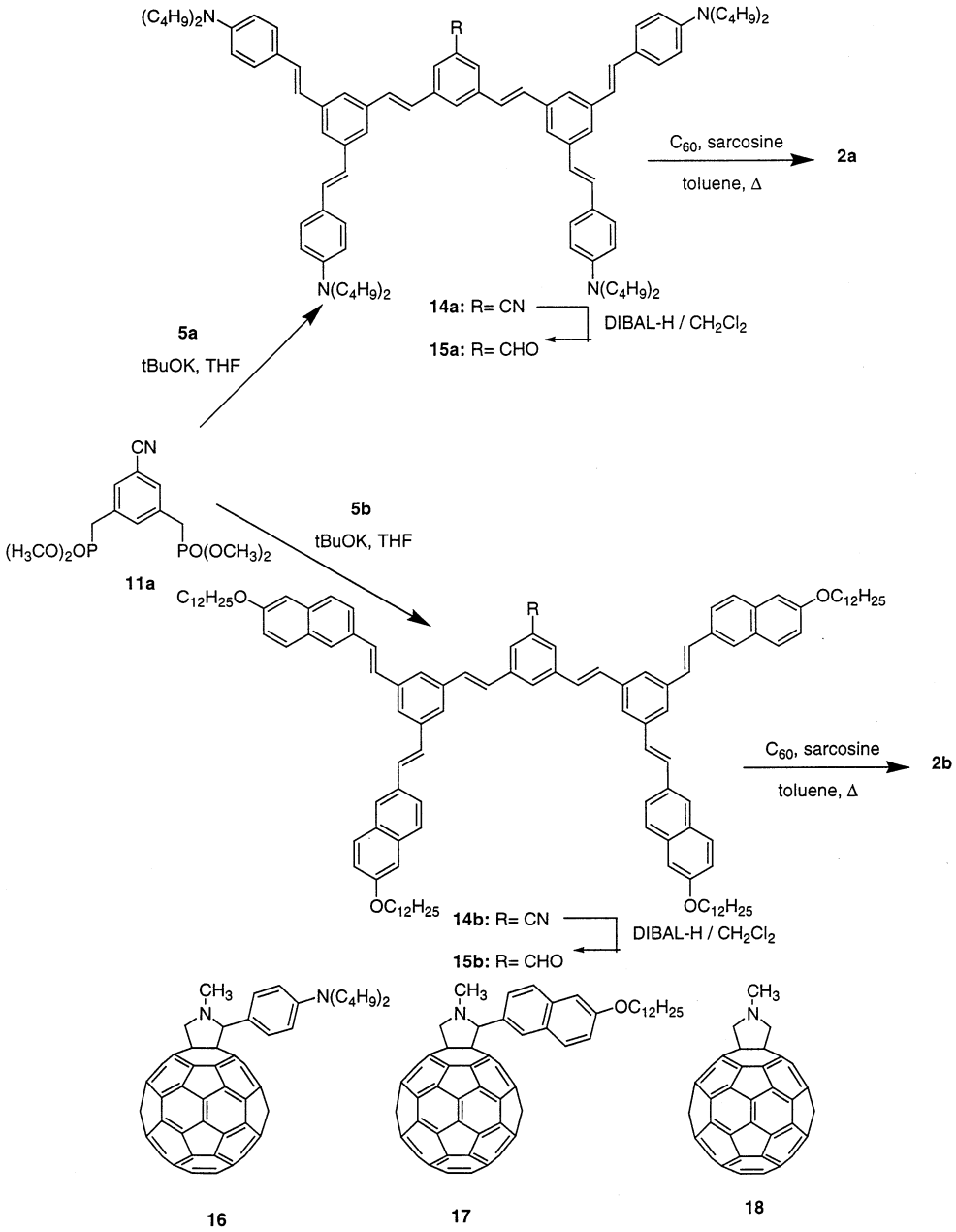

chains, these dyads are quite soluble in common organic solvents.

In $CDCl_3$ solutions, the ^1H NMR spectra of **1a**, **1b**, **2a**, and **2b** confirm that the stereochemistry of the vinylenic double bonds remains unaffected during the cycloaddition reaction ($J_{trans} \sim 16$ Hz). The fulleropyrrolidine signals appear at around 5 ppm (CH) as a singlet and a set of two doublets (CH_2) with coupling constants around $J = 9$ Hz, integrating for one hydrogen. On the other hand, the ^{13}C NMR spectra show the signals originating from the rigid stilbenoid dendron as well as those from the fullerene system. Specifically, in addition to the characteristic fullerene sp^2-region, another four signals, which correspond to the sp^3-carbon atoms of the fulleropyrrolidine ring, were noted between 69 and 84 ppm, and those of the alkoxy chains, between 70 and 15 ppm.

As suitable model systems for the photophysical studies, **16**, **17**, and **18** (Scheme 2) were synthesized by using similar cycloaddition reactions between C_{60} and aldehydes **9**, **12**, and formaldehyde, respectively.

Electronic Absorption Spectra. The absorption maxima in dichloromethane solutions of the formyl-substituted dendrons (**5a**,**b** and **15a**,**b**) and the respective dyads (**1a**,**b** and **2a**,**b**) are given in Table 1 along with references **16**−**18**. In general, the values for the dibutylaniline derivatives are around 370−380 nm, whereas the analogues bearing the alkoxynaphthalene moiety appear at around 336−340 nm. A red shift is observed in the λ_{max} values in dibutylaniline derivatives in comparison with the parent distyrylbenzene ($\lambda_{max} = 360$ nm) because of the presence of the dialkylamino substituents.

It is interesting to note that substitution of the fullenere unit by the formyl group in the dibutylaniline derivatives results in a slight hypsochromic shift, and the same effect is observed in going from the first to the second dendron generation in dyads **1a** ($\lambda_{max} = 377$ nm) and **2a** ($\lambda_{max} = 369$ nm). A similar effect

Table 1. Absorption Maxima[a] and Redox Potentials[b] of Reference Dendrons (**5a**, **5b**, **15a**, **15b**) and of Dyads (**1a**, **1b**, **2a**, **2b**, **16**, **17**, **18**)

	λ_{max}[a] [nm]	E^1_{ap}[c] [V]	E^1_{cp}[d] [V]	E^2_{cp} [V]	E^3_{cp} [V]	E^4_{cp} [V]
5a	382	+0.88				
1a	377	+0.70	−0.67	−1.08	−1.67	−2.16
15a	373	+0.79				
2a	369	+0.72	−0.73	−1.07	−1.69	
5b	338	+1.30				
1b	340	+1.27	−0.64	−1.03	−1.62	
15b	336	+1.32				
2b	338	1.30	−0.64	−1.03	−1.62	
16	312	1.08	−0.65	−1.07	−1.64	
17	308		−0.64	−1.04	−1.65	
18	322	1.32	−0.71	−1.14	−1.75	
C_{60}			−0.60	−1.07	−1.64	−1.93

[a] In dichloromethane solutions [b] In toluene−acetonitrile solvent mixture (4:1 v/v) using Bu_4NClO_4 (0.3 mg L^{-1}), SCE reference electrode, and glassy carbon as working electrode. Scan rate: 200 mV s^{-1}. [c] ap: anodic peak. [d] cp: cathodic peak.

was also observed for the respective alkoxynaphthalene derivatives, although to a lesser extent (see Table 1).

Electrochemistry. The electrochemical features of dyads **1a**, **1b**, **2a**, **2b**, **16**, and **17** were probed by cyclic voltammetry at room temperature (see Supporting Information, Figure S1). A toluene−acetonitrile solvent mixture (4:1 v/v) and tetra-*n*-butylammonium perchlorate (0.3 mg/mL) as supporting electrolyte were used in a conventional three-compartment cell, equipped with glassy carbon, SCE, and platinum wire as working electrode, reference electrode, and auxiliary electrode, respectively. The redox potentials, measured at 200 mV s^{-1}, are collected in Table 1 and compared with those of the formyl-substituted stilbenoid dendrons (**5a**,**b** and **15a**,**b**) and unsubstituted fulleropyrrolidine (**18**).

As a general feature, dyads (**1a**,**b** and **2a**,**b**) give rise to three quasireversible one-electron reduction waves that reflect the first three one-electron reduction steps of the fullerene cores. These reduction potential values are shifted to more negative values relative to pristine C_{60}. The underlying cathodic shift stems from the saturation of a double bond of the fullerene core, which, accordingly, raises the lowest unoccupied molecular orbital (LUMO) energy of the resulting fullerene derivative.[11]

Photophysics. Toluene: Fluorescence Spectroscopy. In toluene, the high-energetic fluorescence (∼3.0 eV) exhibited by the reference dendrons (**5a**,**b** and **15a**,**b**), with quantum yields as high as 0.80, is in the corresponding dyads (**1a**,**b** and **2a**,**b**) reduced by up to 3 orders of magnitude (see Tables 2 and 3 and Figure 2a). Taking the fluorescence quantum yields and lifetime of the references into account, we extrapolated the lifetime and, accordingly, the rate of deactivation for the photoexcited dendrimer structure. Details on this determination are listed in the footnote to Table 3. For example, a lifetime of 0.4 ± 0.01 ps is estimated for **1a** in toluene, which corresponds to an ultrafast intramolecular deactivation rate of 2.5×10^{12} s^{-1}. Similar values were determined for **1b**, **2a** and **2b** and are collected in Table 3.

Toluene: Transient Absorption Spectroscopy. Because the synopsis of the emission studies, along with the thermodynamic calculations (vide infra), suggests that an intramolecular singlet−singlet energy transfer occurs, further examination of these fullerene-based dendrons was deemed necessary. This led us to characterize the photophysics of reference dendrons (**5a**,**b** and **15a**,**b**) by transient absorption changes, recorded with several time delays after a short picosecond (Figure 3a) and long nanosecond (Figure 3b) laser pulse, and compare them to those of the corresponding dyads (**1a**,**b** and **2a**,**b**) (Figure 4).

Table 2. Photophysical Characteristics of Reference Dendrons (**5a**, **5b**, **15a**, **15b**)

	5b	15b	5a	15a
λ_{max} fluorescence	401 nm[a] (3.09 eV)	408 nm[a] (3.03 eV)	468 nm[b] (2.65 eV)	454 nm[b] (2.72 eV)
Φ fluorescence	0.8	0.47	0.17	0.31
τ fluorescence	1.76 ns[c]	1.99 ns[c]	1.95 ns[c]	2.05 ns[c]
λ_{max} singlet−singlet[d]	600 nm	680, 950 nm	650, 945 nm	645, 945 nm
τ singlet[d]	1.85 ns[e]	1.97 ns[e]	1.90 ns[e]	2.01 ns[e]
λ_{max} triplet−triplet[d]	380, 580 nm	390, 590 nm	620 nm	680 nm
λ_{max} π-radical cation[f]	510 nm	540 nm	480, 820 nm	480, >900 nm

[a] Excitation wavelength 340 nm. [b] Excitation wavelength 380 nm. [c] Measured at the fluorescence maximum, see entry 1. [d] Excitation wavelength 355 nm. [e] Measured at the singlet−singlet maximum, see entry 4. [f] Determined by pulse radiolysis.

We turn first to the question of the reference dendrons (**5a**,**b** and **15a**,**b**). At early times (i.e., 50−100 ps), characteristically strong transitions, which are short-lived ($\tau \sim 2$ ns), were found in the visible region (600−750 nm). Photoexcitation of, for example, **15b** (2.0×10^{-5} M) led to the instantaneous formation of a broad ∼680 nm maximum, which is ascribed to the singlet excited-state absorption feature. A representative spectrum, monitored with a 50 ps time delay, is given in Figure 3a. At longer times, the singlet excited state deactivates via a mono-exponential rate law and a rate of 5.0×10^8 s^{-1} to produce the long-lived triplet excited state (Figure 3a, 5000 ps time delay).[12] Similar properties were concluded for **5a**,**b** and **15a** in toluene.

In nanosecond experiments, **15b** gave rise to spectral features shown in Figure 3b. The spectrum, representative of **5a**,**b** and **15a**, displays maxima between 580 and 680 nm. Analysis of the transient absorption changes throughout the 550−950 nm region reveals a reasonably good spectral correlation with what is seen to develop over the course of the picosecond time regime. The triplet absorbances of **5a**,**b** and **15a** generally decayed via dose-independent first-order kinetics and resulted in a complete restoration of the ground state.

$$\text{dendron} \xrightarrow{h\nu} {}^1\text{*(dendron)} \xrightarrow{\text{ISC}} {}^3\text{*(dendron)} \qquad (1)$$

The picture associated with the picosecond absorption spectroscopy of dyads **1a**,**b** and **2a**,**b** is drastically different from the conclusion of reference dendrons **5a**,**b** and **15a**,**b**. Despite the unequivocal excitation of the dendrimer moieties ($\lambda_{ex} = 355$ nm), no spectral evidence for the dendrimer's singlet−singlet absorption was found at any delay time following the short 18 ps laser pulse. Instead, the spectral features are identical with

(11) (a) Suzuki, T.; Maruyama, T.; Akasaba, T.; Ando, W.; Kobayashi, K.; Nagase, S. *J. Am. Chem. Soc.* **1994**, *116*, 1359. (b) Chlistouff, J.; Cliffel, D.; Bard, A. J. In *Handbook of Organic Conductive Molecules and Polymers Vol. 1*; Nalwa, N. S., Ed.; John Wiley & Sons: New York, 1997; Chapter 7. (c) Echegoyen, L.; Echegoyen, L. E. *Acc. Chem. Res.* **1998**, *31*, 593.

(12) It is worthwhile to underline that these intersystem crossing (ISC) kinetics reveal an almost exact resemblance with those of the fluorescence lifetime (see Table 2).

Table 3. Photophysical Characteristics of Dyads (**1a**, **1b**, **2a**, **2b**, **16**, **17**)

	17	1b	2b	16	1a	2a
			Dendron			
Φ fluorescence (toluene)		1.8×10^{-4} [a]	3.2×10^{-3} [a]		2.7×10^{-4} [b]	2.5×10^{-3} [b]
Φ fluorescence (THF)		1.6×10^{-4} [a]	3.0×10^{-3} [a]		1.9×10^{-4} [b]	2.2×10^{-3} [b]
τ fluorescence (toluene)[c]		0.4 ± 0.01 ps	13 ± 0.1 ps		3 ± 0.03 ps	16 ± 0.1 ps
			Fullerene			
Φ fluorescence (toluene)	6.0×10^{-4} [a]	5.6×10^{-4} [a]	5.4×10^{-4} [a]	5.9×10^{-4} [b]	1.6×10^{-4} [b]	3.9×10^{-4} [b]
Φ fluorescence (THF)		4.3×10^{-4} [a]	4.0×10^{-4} [a]	0.2×10^{-4} [b]	0.2×10^{-4} [b]	0.6×10^{-4} [b]
Φ fluorescence (benzonitrile)		3.4×10^{-4} [a]	3.0×10^{-4} [a]	0.15×10^{-4} [b]	0.15×10^{-4} [b]	0.5×10^{-4} [b]
τ fluorescence (toluene)	1.5 ns	1.42 ns	1.51 ns	1.38 ns		1.48 ns
τ fluorescence (THF)	1.44 ns	1.39 ns	1.40 ns	nd[d]	nd[d]	nd[d]

[a] Excitation wavelength 340 nm. [b] Excitation wavelength 380 nm. [c] Calculated values according to $k = [\Phi(\text{ref}) - \Phi(\text{dyad})]/[\tau(\text{ref})\Phi(\text{dyad})]$. [d] Not detectable; lifetimes shorter than the time resolution of our apparatus (i.e., ~ 0.1 ns).

the texture of the fullerene singlet excited state. Specifically, a broad transition centering around 880 nm is a clear attribute of the fullerene singlet−singlet absorption, as illustrated in Figure 4a.[13] As can be seen by reference to Figure 4b, which displays time profiles taken in toluene and benzonitrile, the fullerene singlet excited state is formed instantaneously and in a single step. The rise time of the 880 nm absorption, as a sensitive marker for the actual energy-transfer event, is masked by the instrument response time and, therefore, prevents an accurate kinetic analysis of the intramolecular reaction, but it allows us to estimate a lower limit, $>5 \times 10^{10}$ s^{-1}.[14] In principle, this estimate corroborates the ultrafast deactivation, as we extrapolated from the fluorescence experiments (vide supra). On the longer time scale, the fate of the fullerene singlet excited state is identical to that found for fulleropyrrolidine **18**: An ISC (intersystem crossing) ($\sim 5 \times 10^8$ s^{-1}), driven by a strong spin−orbit coupling, governs the efficient transformation of the singlet into the triplet excited state with λ_{max} at 700 nm.

THF and Benzonitrile: Fluorescence Spectroscopy. When more polar solvents, such as THF and benzonitrile, were used, the steady-state fluorescence experiments (Table 3) gave rise to several interesting trends.

First, the high-energetic dendrimer emission decreases in all systems (**1a**,**b** and **2a**,**b**) by about 10% in comparison to the experiments conducted in nonpolar toluene.

Second, in the dodecyloxynaphthalene-based systems (**1b**, **2b**), the fullerene fluorescence drops in benzonitrile by 45% (3.0×10^{-4}) relative to that in toluene (5.4×10^{-4}). This observation is consistent with the assumption that a competing electron transfer may be activated (vide infra).[15]

Third, and most importantly, in the dibutylaniline-based systems (**1a**, **2a**), the quantum yields of the fullerene fluorescence were as low as 0.15×10^{-4} (**1a** in benzonitrile).

THF and Benzonitrile: Transient Absorption Spectroscopy. Upon 355 nm illumination (18 ps) of **1a**,**b** and **2a**,**b** in THF and benzonitrile, the typical fullerene singlet−singlet absorptions were seen, similar to the trend realized in toluene (vide supra, compare to Figure 4).[16]

Interestingly, for **1b** and **2b**, no obvious impact on the singlet lifetime was noted: The monoexponential rates ($\sim 6 \times 10^8$ s^{-1}), as summarized in Table 4, are virtually identical, although the fullerene fluorescence quantum yields drop to 50%.[17] For example, in Figure 4b, the time absorption profiles at 880 nm are compared for dyad **2b** in oxygen-free toluene and benzonitrile. At the conclusion of the picosecond time scale, the only recognizable product is the fullerene triplet excited state, judged by the 700 nm triplet−triplet absorption, with a triplet lifetime of ~20 μs.

The fluorescence experiments led us to postulate that in the dibutylaniline-based systems **1a** and **2a** the lifetimes of the fullerene singlet excited states are strongly affected by the electron donor. In fact, transient absorption measurements disclosed that the slow intersystem crossing dynamics (7.4×10^8 s^{-1}) do not govern the lifetime of the fullerene singlet excited state but that a rapidly occurring decay of the singlet−singlet transition does. Figure 6 illustrates the decay at the 880 nm maximum of **2a** in toluene and THF.

The transient absorption changes, recorded at the conclusion of this fast deactivation, are not superimposable with those

(13) The slightly lower fluorescence quantum yield can be correlated with the better electron-donor ability of dibutylaniline dendrons (**5a**, **15a**) relative to the dibutylaniline moiety in **16**.

(14) Similar rise and decay kinetics were found upon analyzing at alternative wavelengths in the near-infrared region.

(15) Earlier, we noticed a similar trend in fullerene−oligomer ensembles, see ref 35c.

(16) We like to emphasize that again the transduction of singlet excited-state energy (eq 1) precedes the fullerene singlet excited-state information. This process is covered by our instrumental time response of 18 ps. See also previous discussion on toluene.

(17) Similarly, the fullerene fluorescence lifetimes are identical.

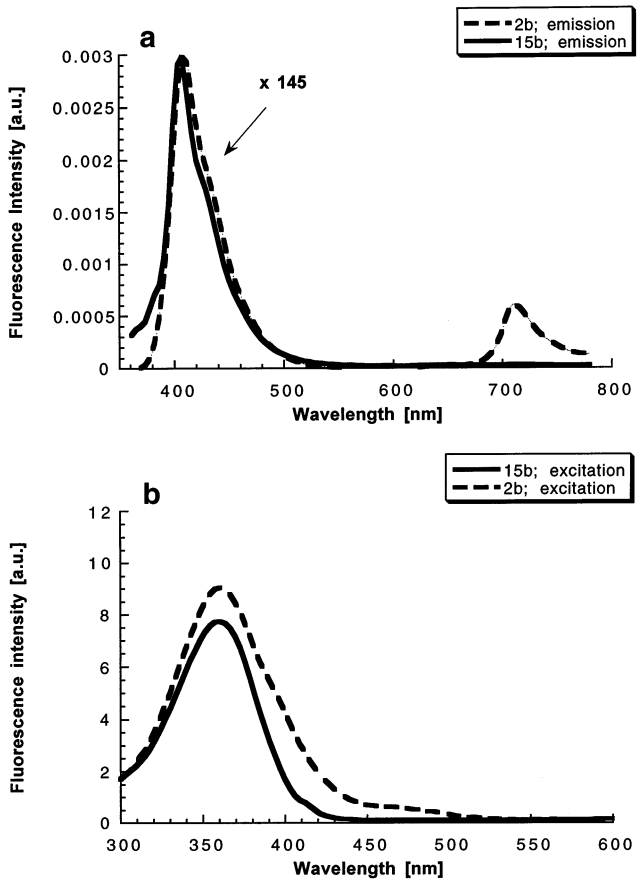

Figure 2. (a) Emission spectra of dyad **2b** and reference **15b** in toluene with matching absorption at the 340 nm excitation wavelength (i.e., $OD_{340\ nm} = 0.2$) (emission spectrum of dyad **2b** is amplified by a factor of 145) and (b) excitation spectra (normalized to exhibit matching signals around 350 nm) of dyad **2b** in toluene and reference **15b** in toluene, monitoring the fullerene emission at 715 nm and dendron emission at 410 nm, respectively.

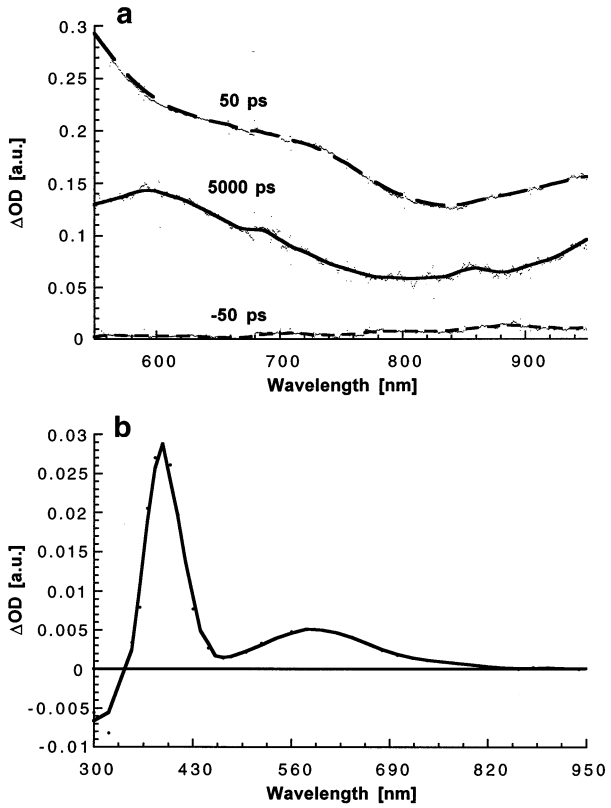

Figure 3. (a) Picosecond transient absorption spectrum (vis−NIR part) recorded −50 ps, 50 ps (- - -), and 5000 ps (—) upon flash photolysis of reference **15b** (5.0×10^{-5} M) at 355 nm in deoxygenated toluene, indicating the dendron singlet−singlet ($\lambda_{max} = 680$, 950 nm) and triplet−triplet features ($\lambda_{max} = 590$ nm), respectively. (b) Nanosecond transient absorption spectrum (vis−NIR part) recorded 50 ns upon flash photolysis of reference **15b** (5.0×10^{-5} M) at 355 nm in deoxygenated toluene, indicating the dendron triplet−triplet features ($\lambda_{max} = 390$, 590 nm).

recorded for the fullerene model, that is, the fullerene triplet excited state ($\lambda_{max} \sim 380$ and 700 nm).[18] Instead, the newly formed species shows a sharp peak around 1000 nm, the characteristic fingerprint of the one-electron reduced fullerene π-radical anion. As far as the dibutylaniline moieties are concerned, transient maxima in the visible around 820 nm corroborate the oxidation of the donor and complete the characterization of the charge-separated $C_{60}^{\bullet-}$ −dendron$^{\bullet+}$ radical pairs. Using the comparative method and the fullerene triplet as a standard, quantum yields of the charge separation as high as 0.76 were derived in dichloromethane. It is interesting to note that in **1a** and **2a** $C_{60}^{\bullet-}$ −dendron$^{\bullet+}$ is the only product formed: no evidence for a long-lived excited state was seen at any time delay.

Discussion

Synthesis. The first approach involves Wittig reaction between 1,3,5-triformylbenzene (**3**) and *p*-(*N*,*N*-dibutylamino)-benzylphosphonium derivative **4** under stoichiometric control. The disadvantage of this approach is that compound **5a** was isolated as a stereoisomeric mixture. Transforming the stereoisomers into the pure *E*,*E* isomer necessitated refluxing the material in *p*-xylene in the presence of catalytic amounts of iodine. Trialdehyde (**3**) was obtained following a two-step reaction sequence: Reduction of the commercially available methyl 1,3,5-benzenetricarboxylate to the corresponding tri-(hydroxymethyl) derivative and oxidation with pyridinium chlorochromate.[19] On the other hand, synthesis of 4-(*N*,*N*-dibutylamino)benzyltriphenylphosphonium iodide (**4**) was completed via treatment of *N*,*N*-dibutylaniline with triphenylphosphine, potassium iodide, and formaline.[20]

The preparation of 3,5-bis(triphenylphosphoniummethyl)-benzonitrile (**8**) and the related bis(phosphonate) **11a** emerged as a valuable alternative. In particular, radical bromination of 3,5-dimethylbenzonitrile led to the corresponding 3,5-di(bromomethyl)benzonitrile (**7a**),[21] and, upon treatment with triphenylphosphine in dimethylformamide, to derivative **8**. Alternatively, treating **7a** with an excess of trimethyl phosphite afforded the corresponding bis(phosphonate) **11a** (84% yield) as a stable white solid. Upon Wittig reaction between **8** and 4-(*N*,*N*-dibutylamino)benzaldehyde (**9**) in dry ethanol, using lithium ethoxide as a base, **10a** was obtained as a mixture of configurational isomers. Iodine-catalyzed thermal isomerization of the mixture helped to convert **10a** into the pure all-trans isomer. This compound could also be directly separated as the

(18) Guldi, D. M.; Prato, M. *Acc. Chem. Res.* **2000**, *33*, 695.

(19) Formigué, M.; Johannsen, I.; Boubekeur, K.; Nelson, C.; Batail, P. *J. Am. Chem. Soc.* **1993**, *115*, 3752.
(20) Bredereck, H.; Simchen, G.; Gribenow, W. *Chem. Ber.* **1973**, *106*, 3732.
(21) Bodwell, J. G.; Bridsom, J. N.; Houghton, T. J.; Yarlagadda, B. *Tetrahedron Lett.* **1997**, *38*, 7475.

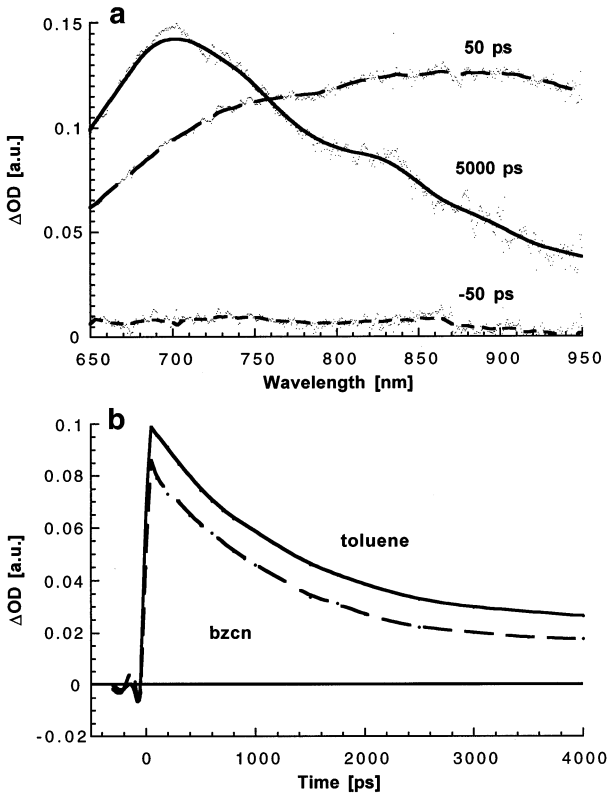

Figure 4. (a) Picosecond transient absorption spectrum (vis−NIR part) recorded −50 ps, 50 ps (- - -), and 5000 ps (—) upon flash photolysis of dyad **2b** (5.0×10^{-5} M) at 355 nm in deoxygenated toluene, indicating the fullerene singlet−singlet ($\lambda_{max} = 880$ nm) and triplet−triplet features ($\lambda_{max} = 700$ nm), respectively. (b) Time−absorption profiles at 880 nm of dyad **2b** in toluene (1.49 ns) and benzonitrile (1.42 ns) monitoring the fullerene singlet−singlet decay (χ^2-values for a monoexponential fit were 0.98 and 0.95 in toluene and benzonitrile, respectively).

pure all-trans isomer, in 67% yield, by Wittig−Horner reaction between bis(phosphonate) **11a** and aldehyde **9** in dry THF at 0 °C, using potassium *tert*-butoxide as a base. Final treatment of a dichloromethane solution of **10a** with a stoichiometric amount of 1.0 M solution of DIBAL-H in dichloromethane then afforded **5a** in a 73% yield as the pure all-trans isomer.

Because of the enhanced fluorescent properties exhibited by naphthalenevinylene derivatives,[22] we have also carried out the synthesis of first- and second-generation dendrons bearing dodecyloxynaphthalene moieties on the peripheral positions as depicted in Schemes 1 and 2.

Radical bromination of 3,5-dimethylbromobenzene (**6b**) yielded 3,5-di(bromomethyl)bromobenzene (**7b**)[23] and, upon heating with trimethyl phosphite, bis(phosphonate) **11b**. Subsequent Wittig−Horner reaction between **11b** and 2-dodecyloxy-6-formylnaphthalene (**12**)[24] allows us to isolate the first-generation dendron, endowed with a bromine atom at the focal point (**13**). The Rosenmund von Braun reaction[25] of bromo derivative **13**, namely, the treatment with copper cyanide in dry *N*,*N*-dimethylformamide in the presence of a catalytic amount of sodium iodide, was then performed en route to the cyano analogue (**10b**). By following a similar strategy as that previously described for the dibutylaniline-containing analogues, aldehyde-functionalized first- and second-generation dendrons were obtained. Subsequent reaction of **5b** with bis(phosphonate) **11a** yielded the cyano-substituted second-generation dendron **14b**, which upon further reduction with DIBAL-H leads to the second-generation dendron **15b** (Scheme 2).

Table 4. Photophysical Characteristics, Related to the Fullerene Features, of Dyads (**1a**, **1b**, **2a**, **2b**, **16**)

	1b	2b	16	1a	2a
τ singlet (toluene)	1.59 ns	1.49 ns	1.55 ns	0.73 ns	1.40 ns
τ singlet (THF)	1.50 ns	1.51 ns	0.04 ns	0.05 ns	0.16 ns
τ singlet (benzonitrile)	1.47 ns	1.42 ns		0.03 ns	0.09 ns
Φ triplet (toluene)	0.79	0.6		0.15	0.29
Φ triplet (THF)	0.69	0.43		radical pair Φ 0.47	radical pair Φ 0.41
Φ triplet (DCM)[a]				radical pair Φ 0.74	radical pair Φ 0.76
Φ triplet (benzonitrile)	0.59	0.3		radical pair Φ 0.53	radical pair Φ 0.46
τ radical pair (THF)	triplet	triplet		220 ns	350 ns
τ radical pair (DCM)[a]				250 ns	580 ns
τ radical pair (benzonitrile)	triplet	triplet		360 ns	725 ns

[a] DCM = dichloromethane.

Electronic Spectra and Electrochemistry. The ground-state absorption spectra of all dyads are a superposition of the spectra of the individual chromophores. However, the λ_{max} values in the dyads are hypsochromically shifted relative to those of the respective formyl-substituted dendrons, which could be accounted for by the loss of conjugation in going from the carbonyl group to the fullerene unit. More fundamental is the observation that the higher generations exhibit enhanced absorption cross sections. For example, extinction coefficients of 3680 M^{-1} cm^{-1} (**5a**) and 7800 M^{-1} cm^{-1} (**15a**) of the visible transition (i.e., ~380 nm) clearly parallel the increase of light-absorbing units, thus giving rise to a useful antenna effect.

A closer inspection of the electrochemical data reveals that the first reduction potential values of these dyads are all very similar (see Table 1). Furthermore, they compare quite well with that of the fulleropyrrolidine reference (**18**) in which the same double bond of the fullerene core is saturated.

The redox behavior of the stilbenoid dendrons shows an increase of the donor strength when going from the dodecyloxynaphthalene-based (**5b**, **15b**: $E_{ox} \sim 1.30$ V vs SCE) to the dibutylaniline-based systems (**5a**, **15a**: $E_{ox} \sim 0.7$ V vs SCE). This fact is in agreement with the better donor ability of the

(22) (a) Segura, J. L.; Martín, N.; Hanack, M. *Eur. J. Org. Chem.* **1999**, 643. (b) Döttinger, S. E.; Hohloch, M.; Segura, J. L.; Steinhuber, E.; Hanack, M.; Tompert, A.; Oelkrug, D. *Adv. Mater.* **1997**, *9*, 233. (c) Hohloch, M.; Segura, J. L.; Döttinger, S. E.; Hohnholz, D.; Steinhuber, E.; Spreitzer, H.; Hanack, M. *Synth. Met.* **1997**, *84*, 319.
(23) (a) Steenwinkle, P.; James, S. L.; Grove, D. M.; Veldman, N.; Speck, A. L.; van Koten, G. *Chem.—Eur. J.* **1996**, *2*, 1440. (b) Paugan, M. F.; Bien, J. T.; Smith, B. D.; Christoffels, L. A. J.; Dejong, F.; Reinhoudt, D. N. *J. Am. Chem. Soc.* **1996**, *118*, 9820.
(24) Gómez, R.; Segura, J. L.; Martín, N. *J. Org. Chem.* **2000**, *65*, 7501.
(25) Ellis, G. P.; Romney-Alexander, T. M. *Chem. Rev.* **1987**, *87*, 779.

dibutylaniline group in comparison with that of dodecyloxynaphthalene.[26]

In summary, both electronic spectra and electrochemical data reveal the absence of a significative interaction between the C_{60} and electron donor units in the ground state.

Photophysics: Toluene. Inspection of the low-energy region of the emission spectra (see Figure 2a) helped to identify the species evolving from the dendrimer's singlet excited-state quenching in **1a**,**b** and **2a**,**b** and, furthermore, to probe the underlying mechanism. In particular, a fluorescence maximum at 715 nm, resembling that of fulleropyrrolidine **18**,[18] was produced, despite the near exclusive excitation of the dendron moieties at 360 nm (≫90%).[27] The fact that we realize nearly comparable quantum yields, relative to that of reference **18**, lets us conclude that the fullerene singlet excited state (1.76 eV) is populated in quantitative yields. Evidence that this newly formed state is produced from an energy-transfer reaction, rather than evolved from a direct excitation, was lent from a set of excitation spectra. The complementary excitation spectrum of the fullerene emission in dyads **1a**,**b** and **2a**,**b** (Figure 2b) reflects nearly exactly (i) the ground-state absorption of the dendron moieties in the near-visible region and (ii) the excitation spectra of **5a**,**b** and **15a**,**b** with maxima ∼ 350 nm. These analyses underscore the hypothesis that the origin of excited state energy is unequivocally that of the dendron systems.

$$C_{60}\text{–dendron} \xrightarrow{h\nu} C_{60}\text{–}^{1}\text{*(dendron)} \rightarrow {}^{1}\text{*}(C_{60})\text{–dendron} \quad (2)$$

To correlate this interesting phenomenon, we examined references **16** (dibutylaniline-based system) and **17** (dodecyloxynaphthalene-based system),[28] under nearly identical conditions. The high-energy regime of the naphthalene-based system (**17**) is dominated by a significant quenching (∼97%) of the dodecyloxynaphthalene emission, while in the low-energy region the fullerene fluorescence appears. Because the dibutylaniline group in **16** lacks the strong absorption seen in the dendron analogues **5a**, **15a**, **1a**, and **2a**,[29] only the fullerene fluorescence was probed (Table 3). Although the fullerene fluorescence quantum yields are in both systems (i.e., **16**,**17**) comparable to that of fulleropyrrolidine reference **18**, different conclusions are evoked. In the naphthalene-based system (**17**), it confirms a quantitative transfer of singlet excited-state energy from the dodecyloxynaphthalene unit to the fullerene, in sound agreement with the corresponding dendrons (**1b**,**2b**). On the other hand, in **16**, it only infers that any energy transferred to the fullerene remains there and an intramolecular electron evolving from the fullerene singlet excited state is thermodynamically precluded. This conclusion agrees well with the thermodynamic argument suggesting an endothermic electron transfer in toluene, $-\Delta G < 0$ (vide infra).[13]

As a final test in support of the energy-transfer hypothesis, the triplet characteristics (i.e., triplet–triplet maximum, lifetime and quantum yield) were compared in nanosecond experiments, as an example, following 8 ns pulses at 355 nm. First, the triplet–triplet maxima (Figure 5) were in perfect accord with the spectral features observed at the end of the picosecond time scale (compare to Figure 4). Second, the triplet lifetimes (ca. 20 μs) match those seen for reference **18**.

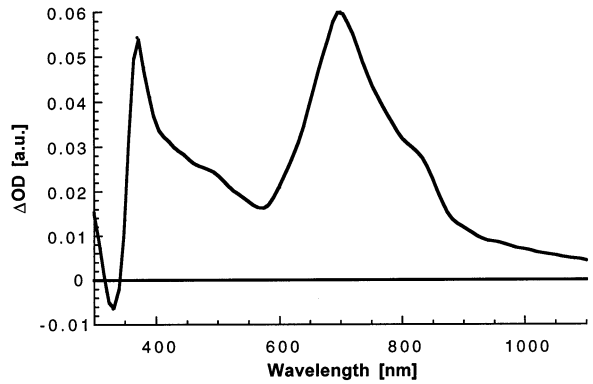

Figure 5. Nanosecond transient absorption spectrum (vis–NIR part) recorded 50 ns upon flash photolysis of dyad **2b** (5.0×10^{-5} M) at 355 nm in deoxygenated toluene, indicating the fullerene triplet–triplet features (λ_{max} = 380, 700 nm).

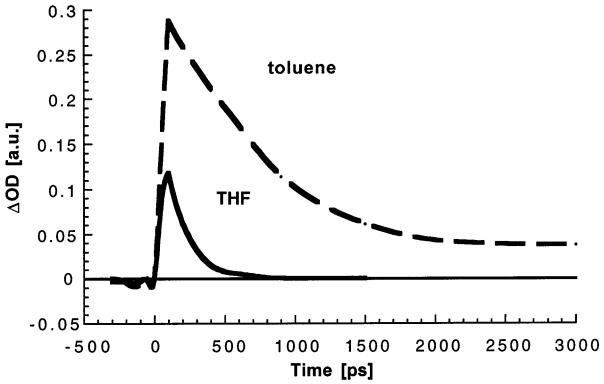

Figure 6. Time–absorption profiles at 880 nm of dyad **2a** in toluene (1.40 ns) and THF (0.16 ns) monitoring the fullerene singlet–singlet decay (χ^2-values for a monoexponential fit were 0.98 and 0.99 in toluene and THF, respectively).

As far as the references **16** and **17** are concerned, pumping light into the fullerene ground state in **16** leads to the population of the singlet excited state. The lifetime of this intermediate state is, however, not seemingly impacted by the presence of the electron-donating dibutylaniline group. Instead, the lowest vibrational state of the singlet excited state in **16** decays rapidly and quantitatively to the energetically lower lying triplet seen in reference **18**. Furthermore, the differential absorption changes, recorded immediately after an 8 ns pulse, showed the same spectral features of the fullerene triplet excited state as observed at the end of the picosecond experiments. A set of maxima located at 380 and 700 nm was observed, which is in good agreement with the features recorded for **18**.[30]

Photophysics: THF and Benzonitrile. Again, **16** (i.e., dibutylaniline-based system) renders a particularly important reference: Its reactivity assists in shedding light on the mechanism, which might be applicable in deactivating the photoexcited dendron moieties in **1a** and **2a**. In fact, reference **16** reveals a similar low fullerene fluorescence quantum yield,

(26) The presence of a formyl group on the stilbenoid moiety in **5a** and **15a** has a stronger impact on the oxidation potentials than the nonconjugated fullerene unit in **1a** and **2a**. Therefore, the anodic peaks appear in **5a** and **15a** anodically shifted relative to those of **1a** and **2a**. This electronic effect is also observed in the naphthalene derivatives (**5b**, **15b**) although to a notably lesser extent.

(27) Reference dendrons (**5a**,**b** and **15a**,**b**) did not show any emission in this spectral region, see Figure 2a.

(28) Williams, R. M.; Zwier, J. M.; Verhoeven, J. W. *J. Am. Chem. Soc.* **1995**, *117*, 4093.

(29) This hampered the direct excitation of the donor, and only the fullerene emission was subjected to this reference experiment.

(30) A similar reactivity was found for **17**.

for example, in benzonitrile (0.15×10^{-4}). Considering that the singlet and triplet excited-state energies of aniline derivatives are 3.7 ± 0.1 and 3.0 ± 0.1 eV,[31] respectively, energy transfer from the fullerene singlet excited state (1.76 eV) in **16** would be highly endothermic and, therefore, improbable to take place. Consequently, this leaves a very rapid intramolecular electron transfer as the only likely pathway. In fact, in earlier work, it was shown that **16** shows photoinduced electron transfer only in polar media.[28] From this comparison, we reach the tentative conclusion that the fullerene singlet excited state, if produced in the dibutylaniline-based systems (**1a**, **2a**), would be subject to an intramolecular electron transfer.

$$C_{60}-\text{dendron} \xrightarrow{h\nu} C_{60}-{}^1*(\text{dendron}) \rightarrow {}^1*(C_{60})-\text{dendron} \rightarrow C_{60}{}^{\bullet-}-\text{dendron}^{\bullet+} \quad (3)$$

By contrast, in dodecyloxynaphthalene-based systems **1b** and **2b**, this sequential pathway (i.e., transfer of singlet excited-state energy followed by that of an electron, eq 3) plays no major role. The only conceivable rationale for the moderate fluorescence quenching of ~45% might involve a competitive scenario, that is, a direct electron transfer from the photoexcited dendron.

$$C_{60}-\text{dendron} \xrightarrow{h\nu} C_{60}-{}^1*(\text{dendron}) \rightarrow C_{60}{}^{\bullet-}-\text{dendron}^{\bullet+} \quad (4)$$

Correlating the transient absorption experiments for **1b** and **2b** with the emission data, we gather that an intramolecular electron transfer competes (i.e., eq 4) with the dominant singlet−singlet energy transfer (i.e., eq 1). In the context of confirming the electron-transfer contribution, the strong triplet−triplet absorption, which largely dominates the pico- and nanosecond spectra, necessitated its subtraction from, for example, the nanosecond spectrum. Indeed, the corrected spectra (Figure 8) revealed the following characteristics of the $C_{60}{}^{\bullet-}-\text{dendron}^{\bullet+}$ radical pair: The fullerene π-radical anion displayed its typical NIR-fingerprint absorption at 1000 nm plus a maximum around 400 nm,[32] while the one-electron oxidized form of the dendrimers was evidenced through its strong absorption in the visible with maxima around 510 (**1b**) and 540 nm (**2b**).[33] On the basis of the relative yields of triplet versus radical pair, we approximate the quantum yield of charge separation in benzonitrile to be ~10%.

Photophysics: Charge Recombination. Both fingerprints (i.e., ~820 and 1000 nm) were employed as reliable probes, to determine the lifetime of the associated $C_{60}{}^{\bullet-}-\text{dendron}^{\bullet+}$ state in **1a** and **2a** (see Table 4 and Figure 7). The decay curves were well-fitted by a single-exponential decay component. In particular, lifetimes that are on the order of hundreds of nanoseconds (220−725 ns) were derived from the decays of the oxidized donor and reduced acceptor absorptions at 820 and 1000 nm, respectively.[34] The larger donor−acceptor separation in **2a** (16.7 Å), relative to **1a** (11.5 Å), decelerates the charge-recombination dynamics. The dependence of charge-recombination rates versus free energy changes indicates stabilizing effects for the charge-separated state in solvents of higher polarity in both systems. These are clear attributes describing the normal region of the classical Marcus parabola, in sound agreement with the thermodynamic considerations (vide infra).

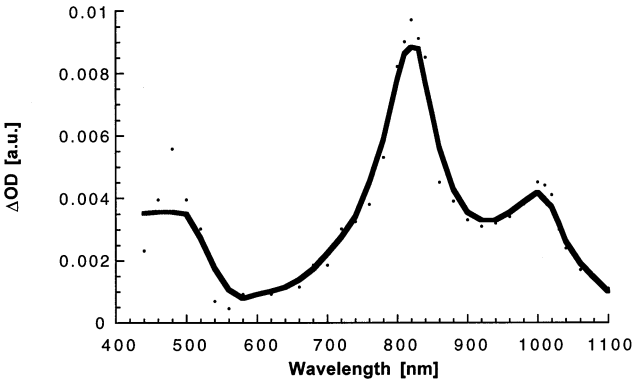

Figure 7. Transient absorption spectrum (vis−NIR part) recorded 50 ns upon flash photolysis of dyad **2a** (2.0×10^{-5} M) at 355 nm in deoxygenated benzonitrile, indicating the charge-separated radical pair features (λ_{max} at 820 and 1000 nm).

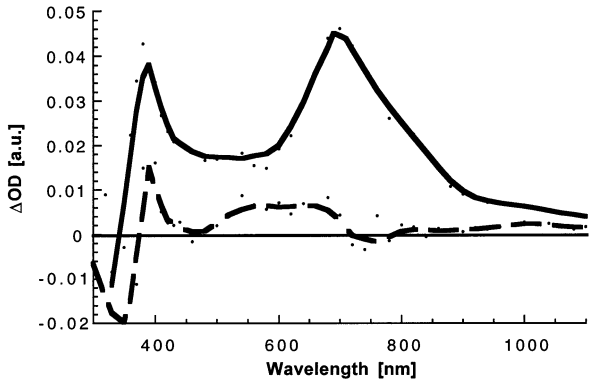

Figure 8. Nanosecond transient absorption spectrum (vis−NIR part) recorded 50 ns upon flash photolysis of dyad **2b** (5.0×10^{-5} M) at 355 nm in deoxygenated benzonitrile before (—) and after (- - -) subtraction of the triplet component.

Thermodynamic Considerations. Upon photoexcitation, an efficient and rapid energy transfer dominates the deactivation of the initially excited dendron moieties in all dyads (i.e., **1a**,**b** and **2a**,**b**). Spectroscopic and kinetic evidence (vide supra) suggests that yet a second contribution, namely, an intramolecular electron transfer, exists.

In dyads **1b** and **2b**, the thermodynamic driving forces (Table 5), associated with an intramolecular electron transfer between the dendron singlet excited state and the fullerene electron acceptor, match the reorganization energies quite well ($-\Delta G_{ET}^{\circ} \sim \lambda$). This leads subsequently to very small $\Delta G_{CS}^{\ddagger}$ values, on the order of 0.004 eV and less. One expected consequence infers that nearly ideal conditions exist for an electron-transfer event, that is, no significant activation barrier. It is nonetheless important to note that the energetic position of the charge-separated state (~1.66 eV) brings it close to that of the fullerene singlet excited state (1.76 eV). Electron transfer evolving from the fullerene singlet excited state in dyads **1b** and **2b** is

(31) Murov, S. L.; Carmichael, I.; Hug, G. L. H*andbook of Photochemistry*; Marcel Dekker, Inc.: New York, 1993.
(32) Guldi, D. M.; Hungerbühler, V.; Janata, E.; Asmus, K.-D. *J. Chem. Soc., Chem. Commun.* **1993**, 84.
(33) The spectral features of the one-electron oxidized products (see Table 2) were charcterized by pulse radiolytic oxidation experiments. This technique was chosen because it is known to be one of the most powerful tools to investigate reactive intermediates, evolving from the selective one-electron transfer, for example, to $[CH_2Cl_2]^{\bullet+}$ and $^{\bullet}OOCH_2Cl/^{\bullet}OOCHCl_2$ peroxyl radicals in oxygenated dichloromethane solutions.
(34) Because of the presence of the bulky substituents, cis−trans isomerization, prior to the rapid deactivation of the dendron singlet excited state (~1 ps), plays no major role.

Table 5. Driving Force Dependence (ΔG_S, $-\Delta G_{CR}°$; $-\Delta G_{CS}°$)[a] and Thermodynamic Parameters (λ; $\Delta G_{CS}^{\ddagger}$)[a] for Intramolecular Electron-Transfer Events and Energy Transfer in Fullerene-Based Dyads (**1a**, **1b**, **2a**, **2b**, **16**, **17**)

		ΔG_S [eV]			$-\Delta G_{CR}°$ [eV]			$-\Delta G_{CS}°$ [c] [eV]			λ [eV]	$\Delta G_{CS}^{\ddagger}$ [eV]	ΔG_{ENERGY} [eV]
	distance[b] [Å]	toluene	THF	bzcn	toluene	THF	bzcn	toluene	THF	bzcn	bzcn	bzcn	
17	R−: 4.4 R_+: 3.5 R_+−: 8.56	0.48	−0.132	−0.328	2.43	1.82	1.62	1.01 (−0.67)	1.58 (−0.07)	1.82 (0.14)	1.16	0.09 (0.22)	1.68
1b	R−: 4.4 R_+: 3.5 R_+−: 14.0	0.78	−0.041	−0.301	2.73	1.91	1.65	0.33 (−0.97)	1.16 (−0.15)	1.41 (0.11)	1.39	0.0001 (0.29)	1.3
2b	R−: 4.4 R_+: 3.5 R_+−: 19.1	0.91	−0.015	−0.288	2.86	1.94	1.66	0.14 (−1.1)	1.06 (−0.18)	1.34 (0.1)	1.49	0.004 (0.32)	1.24
16	R−: 4.4 R_+: 3.7 R_+−: 8.62	0.46	−0.137	−0.32	1.83	1.23	1.05	(−0.07)	(0.53)	(0.71)	1.09	0.033	
1a	R−: 4.4 R_+: 3.7 R_+−: 11.5	0.64	−0.076	−0.306	2.01	1.29	1.06	0.88 (−0.25)	1.6 (0.47)	1.83 (0.7)	1.30	0.06 (0.07)	1.13
2a	R−: 4.4 R_+: 3.5 R_+−: 16.7	0.82	−0.023	−0.288	2.19	1.35	1.08	0.56 (−0.43)	1.4 (0.41)	1.67 (0.68)	1.42	0.01 (0.09)	0.99

[a] See for details: Imahori, H.; Hagiwara, K.; Aoki, M.; Akiyama, T.; Taniguchi, S.; Okada, T.; Shirakawa, M.; Sakata, Y. *J. Am. Chem. Soc*. **1996**, *118*, 11771. [b] (R_+) radius donor; (R−) radius acceptor; (R_+−) donor−acceptor separation. [c] In parentheses, the values are given for intramolecular reactions evolving from the fullerene singlet excited state.

endothermic in toluene and THF and only slightly exothermic in polar benzonitrile. Thus, the thermodynamic conclusion supports the spectroscopic finding: A competition between intramolecular electron transfer and singlet−singlet energy transfer.

The picture is quite different for dyads **1a** and **2a**: Importantly, the charge-separated states are significantly lower in energy (1.06−1.08 eV) than those of the fullerene singlet excited states (1.76 eV). This renders electron transfer from both singlet excited states (i.e., dendron and fullerene) energetically feasible. Considering the calculated free energy changes, $-\Delta G_{ET}°$, of 1.67 eV (**2a**) and 1.83 eV (**1a**) in, for example, benzonitrile, it is clear that they are substantially larger than the reorganization energies ($\lambda \sim 1.40$ eV). Thus, the sequential route in **1a** and **2a** emerges to avoid this strongly exothermic electron transfer, which would be buried deep in the inverted region ($-\Delta G_{ET}° = \lambda$). Instead, the electron transfer occurs from the fullerene singlet ($-\Delta G_{ET}° \sim 0.7$ eV), product of the initial transduction of excited-state energy, and is consequently placed into the normal region.

In summary, variation of the energy gap (see Table 5) modulates the character of the electron-transfer reaction: Depending on the energetic position of the radical pair in reference to the dendron and fullerene singlet excited states, either a competitive or a sequential pathway is activated.

Conclusions

A new convergent route was developed to design a series of C_{60}-based dendrimers carrying dibutylaniline or dodecyloxynaphthalene donors. The dendrimers function as rigid molecular scaffolds, locking the dibutylaniline/dodecyloxynaphthalene electron donors and the fullerene acceptor in spatially well-separated positions. In all dyads, an efficient and rapid energy transfer, as confirmed in a series of steady-state and time-resolved photolytic experiments, dominates the deactivation of the initially excited dendron antennas, generating the fullerene singlet excited state in nearly quantitative yields. A detailed spectroscopic and kinetic analysis prompts, nonetheless, an alternative intramolecular electron transfer, from which an energetic $C_{60}^{\bullet-}$ −dendron$^{\bullet+}$ radical pair evolves. Most importantly, variation of the energy gap modulates the character of this electron-transfer reaction: Depending on the energetic position of the $C_{60}^{\bullet-}$ −dendron$^{\bullet+}$ radical pair, either a competitive (i.e., **1b**, **2b**) or a sequential pathway (i.e., **1a**, **2a**) is activated.

In retrospect, our strategy to devise 1st and 2nd generations of C_{60}−(dendron) ensembles clearly demonstrates that significantly higher absorption cross sections (**2a**,**2b**) and stabilization of an efficiently formed $C_{60}^{\bullet-}$ −dendron$^{\bullet+}$ radical pair (**2a**) are achieved. Considering the overall efficiency of 76% for (i) funneling light from the antenna chromophores to the fullerene core and (ii) charge separation evolving from the fullerene singlet excited state, this model system reproduces natural photosynthesis very well. Clearly, these performances open the way for the preparation of integrated photosynthetic assemblies and photovoltaic devices. Currently, we are pursuing the incorporation of chromophores that absorb more strongly in the visible region of the solar spectrum.

A final comment should address the comparison between C_{60}−dendron dyads and previously investigated C_{60}−oligomer systems.[35−37] First, the meta-linkage of the stilbene units in the dendron breaks the π-conjugation.[38] This allows the control over the effective conjugation length. Second, the rigid dendrons function as efficient mediators for the electron coupling between

(35) (a) Nierengarten, J.-F.; Eckert, J.-F.; Nicoud, J.-F.; Ouali, L.; Krasniko, V.; Hadziioannou, G. *Chem. Commun.* **1999**, 617. (b) Armaroli, N.; Barigelletti, F.; Ceroni, P.; Eckert, J.-F.; Nicoud, J.-F.; Nierengarten, J.-F. *Chem. Commun.* **2000**, 599. (c) Segura, J. L.; Gomez, R.; Martin, N.; Luo, C.; Guldi, D. M. *Chem. Commun.* **2000**, 701. (d) Eckert, J.-F.; Nicoud, J.-F.; Nierengarten, J.-F.; Liu, S.-G.; Echegoyen, L.; Barigelletti, F.; Armaroli, N.; Ouali, L.; Krasnikov, V.; Hadziioannou, G. *J. Am. Chem. Soc.* **2000**, *122*, 7467.
(36) Peeters, E.; van Hal, P. A.; Knol, J.; Brabec, C. J.; Sariciftci, N. S.; Hummelen, J. C.; Janssen, R. A. J. *J. Phys. Chem. B* **2000**, *104*, 10174.
(37) Marcos Ramos, A.; Rispens, M. T.; van Duren, J. K. J.; Hummelen, J. C.; Janssen, R. A. J. *J. Am. Chem. Soc.* **2001**, *123*, 6714.
(38) Additional proof for an intramolecular charge recombination stems from a set of experiments, conducted with different laser power and different dyad concentrations: Decreasing the radical-pair concentration in various increments by up to 65% failed to lead to any notable changes in the charge-recombination kinetics.

electron donor and electron acceptor. As a consequence, highly stabilized and spatially well-separated charge separated states are generated, for example, in **1a** and **2a**, which give rise to a profound distance behavior. Finally, energy transfer dominates the deactivation of photoexcited C_{60}−oligophenylenevinylene dyads[35] with the exception of trimeric/tetrameric α,ω-dimethyl-2,5-bis(2-(*S*)-methylbutoxy)-1,4-phenylene species[36] and polymer with pendant methanofullerenes,[37] for which, however, no quantum yields of charge separation are reported.

Experimental Section

Cyclic voltammograms were recorded on a potentiostat/galvanostat equipped with software for electrochemical analysis by using a GCE (glassy carbon electrode) as working electrode, SCE as reference electrode, Bu_4NClO_4 as supporting electrolyte, toluene and acetonitrile as solvents, and a scan rate of 200 mV/s.

Picosecond laser flash photolysis experiments were carried out with 355 nm laser pulses from a mode-locked, Q-switched Quantel YG-501 DP Nd:YAG laser system (pulse width 18 ps, 2−3 mJ/pulse). Nanosecond laser experiments were performed with laser pulses from a Molectron UV-400 nitrogen laser system (337.1 nm, 8 ns pulse width, 1 mJ/pulse) or from a Qunta-Ray CDR Nd:YAG system (355 nm, 20 ns pulse width). The photomultiplier output was digitized with a Tektronix 7912 AD programmable digitizer. The details of the experimental set-up and its operation have been described elsewhere.[39] The quantum yields of the triplet excited states ($\Phi_{TRIPLET}$) were determined by the triplet−triplet energy-transfer method using β-carotene as an energy acceptor. The quantum yields of the charge separation were measured using the comparative method. In particular, the strong fullerene triplet−triplet absorption ($\epsilon_{700nm} = 16\,100\ M^{-1}\ cm^{-1}$; $\Phi_{TRIPLET} = 0.98$)[40] served as a probe to obtain the quantum yields for the charge-separated state, especially for the fullerene π-radical anion ($\epsilon_{1000nm} = 4700\ M^{-1}\ cm^{-1}$).[41] For all photophysical experiments, an error of 10% must be considered.

Fluorescence lifetimes were measured with a laser strope fluorescence lifetime spectrometer (Photon Technology International) with 337 nm laser pulses from a nitrogen laser fiber-coupled to a lens-based T-formal sample compartment equipped with a stroboscopic detector. Details of the Laser Strobe systems are described on the manufacturer's web site, http://www.pti-nj.com.

Emission spectra were recorded with a SLM 8100 spectrofluorometer. The experiments were performed at room temperature. When measuring the fullerene emission in the 700 nm region, a 570 nm long-pass filter in the emission path was used in order to eliminate the interference from the solvent and stray light for recording the fullerene fluorescence. Each spectrum was an average of at least 5 individual scans, and the appropriate corrections were applied. The fluorescence quantum yields were determined with a 9,10-diphenylanthracene reference (Aldrich, 99+%) ($\Phi = 1$) and an average value of 3 fluorophore concentrations with ODs at the excitation wavelength ranging from 0.1 to 0.5.

All melting points were measured with a melting point apparatus and are uncorrected. FTIR spectra were recorded as KBr pellets. ^{13}C and ^{1}H NMR spectra were recorded with a 300 MHz (for ^{1}H) and 75 MHz (for ^{13}C) spectrometer. Chemical shifts are given as δ values (internal standard: TMS).

3,5-Dimethylbromobenzene (**6b**) and *N*,*N*-dibutylaminobenzaldehyde (**9**) are commercially available and were used without further purification. 1,3,5-Triformylbenzene (**3**),[11] *N*,*N*-dibutylamino-4-(triphenylphosphoniummethyl)benzene iodide (**4**),[20] 3,5-dimethylbenzonitrile (**6a**),[42] 3,5-di(bromomethyl)benzonitrile (**7a**),[13] and 6-dodecyloxy-2-formylnaphthalene (**12**)[23] were obtained by following previously described synthetic procedures. Dichloromethane was distilled from $CaCl_2$, and ethanol was distilled from Mg and iodine.

Acknowledgment. This work has been supported by the DGESIC of Spain (Project BQU2002-00855) and by the European Comission (Contract JOR3CT980206) and the Office of Basic Energy Sciences of the U.S. Department of Energy (Contribution NDRL-4392 from the Notre Dame Radiation Laboratory). We are also indebted to Centro de Espectroscopía de la UCM.

Supporting Information Available: Synthetic section and cyclic voltammetry (PDF). This material is available free of charge via the Internet at http://pubs.acs.org.

JA012694X

(39) Thomas, M. D.; Hug, G. L *Comput. Chem.* **1998**, *22*, 491.
(40) Luo, C.; Fujitsuka, M.; Watanabe, A.; Ito, O.; Gan, L.; Huang, Y.; Huang, C.-H. *J. Chem. Soc., Faraday Trans.* **1998**, *94*, 527.
(41) Luo, C.; Fujitsuka, M.; Huang, C.-H.; Ito, O. *Phys. Chem. Chem. Phys.* **1999**, *1*, 2923.
(42) Gryszkiewicz-Trochimowski, H. M. E.; Schmidt, W.; Gryszkiewicz-Trochimowski, G. T. O. *Bull. Chim. Fr.* **1948**, 593.